

CALIBRATION AND PERFORMANCE ANALYSIS OF THE X-SAR SYSTEM

M. Zink

DLR, German Aerospace Research Establishment
Institute for Radio Frequency Technology
82234 Oberpfaffenhofen, Germany
Phone: +49-8153-28-2386, FAX: +49-8153-28-1449

Abstract

In April 1994 the X-SAR was flown as part of the first SIR-C/X-SAR space radar laboratory mission on the Space Shuttle. Our institute is responsible for the calibration of all X-SAR data products. Before the mission we performed a detailed analysis of the overall system to localize the main error sources and developed algorithms and procedures to correct these errors. During the mission we have been running a rather big calibration campaign. Some 30 colleagues were involved in the deployment and operation of calibration receivers and external reference targets. Post mission activities include the determination of the antenna pattern and the absolute calibration factor as well as detailed performance analyses.

INTRODUCTION

The X-band Synthetic Aperture Radar (X-SAR) is an imaging radar designed to complement the SIR-C L- and C-band systems (Jordan, 1991). It is operated at a frequency of 9.6 GHz under vertical polarization. The shorter wavelength (0.03125 m) of the X-SAR system has particularly favorable capabilities for several applications in the area of vegetation, oceanography, snow/ice and geology. Its weak penetration into the surface and its high sensitivity to surface roughness and associated phenomena can be seen as a significant enhancement to the L- and C-band measurements of SIR-C.

Quantitative analyses of SIR-C/X-SAR data require absolute radiometric calibration of the overall system. Data should be corrected for all power and gain variations and the radiometric modulation in cross-track direction (range dependence and antenna elevation pattern). These corrections have to be done during precision processing. The overall processor gain has to be normalized to be independent of range resolution, PRF, processed bandwidth, and effective number of looks (Bamler, 1993). The absolute calibration factor can be determined from images of calibration sites equipped with external reference targets like corner reflectors and active radar calibrators (ARCs).

In X-SAR calibration we have two main problems (Zink, 1993): the receiver gain drift with temperature and the insufficient knowledge of the antenna boresight direction. The first problem can be solved by using the internal calibration loops to monitor the system gain variations with temperature and time. The other information, which is necessary for radiometric corrections of the cross-track antenna pattern, is the antenna boresight. The SIR-C null-tracker provides the boresight angle of the L- and C-band antennas throughout the whole mission. X-SAR uses this information and measurements of the offset in elevation between SIR-C nulls and X-SAR boresights for different look angles. These offsets can be derived from ground receiver measurements at the Oberpfaffenhofen test site and from images of homogenous distributed targets (rain forest).

This paper includes a detailed description of the X-SAR calibration algorithms and procedures and preliminary results of the first mission.

INTERNAL CALIBRATION

Figure 1 shows a block diagram of the X-SAR system including calibration relevant sub-systems. The chirp signal is generated in the frequency generation unit (FGU) and upconverted to 9.6 GHz in the frequency conversion unit (FCU). After amplification in the high power amplifier (HPA), the signal passes the circulator (C) and is transmitted by the antenna. On receipt, the received power from the antenna goes through the circulator, the shutter (S), the band-pass filter and limiter (FL) into the low noise amplifier (LNA). The signal is amplified in the LNA and the subsequent receiver part (RX), sampled in the analog-digital converter (ADC) and stored on high density digital tapes. The receiver gain is set by a stepped attenuator (in RX) in steps of 2 dB from a maximum total gain of 80 dB down to 40 dB.

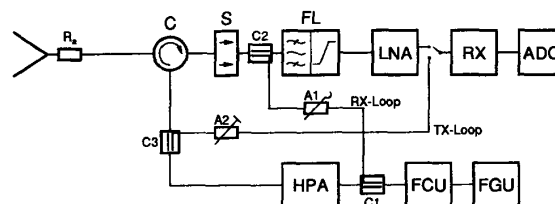


Figure 1: X-SAR block diagram including calibration loops

To monitor essential system parameters (temperature, power, voltage, current) corresponding sensors are installed throughout the whole system. The temperature sensors are located at system elements, where the temperature is representative (e.g. SAW filter for RX temperature). The various sensor data are telemetered down.

The block diagram in figure 1 includes the built-in calibration loops. The TX-calibration coupler (C3) couples out part of the high power transmit signal. This calibration signal (chirp) passes a fixed attenuator (A2) and the receiver (excluding the LNA) and is stored in the raw data stream. The RX-gain for the TX-loop is set to mid gain (60 dB). The RX-calibration uses part of the stable FCU-output (leveled output) and checks the whole receiver dynamic range by stepping the RX-loop attenuator (A1) in steps of 5 dB from 0 to 60 dB (calibration level) and the receiver gain over the whole 40 dB range.

RX- and TX-calibration are performed at the beginning and end of each data take. To take into account variations during a data take, linear interpolation between these two values will be used (Bamler, 1993). The calibration data are formatted like SAR data and stored in the raw data stream.

A first look on these house-keeping data received during the mission indicates very stable output power levels and system temperatures. Detailed analyses concerning the sensor stability will be presented at the symposium.

ANTENNA PATTERN MEASUREMENTS

Adequate radiometric corrections of the SAR data require knowledge of the sensor-target geometry and the antenna elevation pattern. Preflight measurements have been performed on the three separate leaves of the X-SAR slotted wave guide antenna on an antenna test range (Alenia, 1991). The reconstructed pattern has been calculated from the data of the single leaves.

One of the main activities at the Oberpfaffenhofen test site was the verification of the actual inflight antenna pattern using ground calibration receivers (Seifert, 1992). For that purpose we deployed 20 receivers in each frequency band over an area of approximately 100 km extension. Our receivers were designed and manufactured by the Institute of Navigation at the University of Stuttgart.

These instruments are capable of handling various pulse lengths, PRFs, and have a very high dynamic range. The precise internal clocks are synchronized to UTC using GPS receivers. Each radar pulse is sampled sixteen times. The built-in microcomputer stores the measured samples to a maximum of 8000 pulses, sets time marks, and writes the operating temperature and the individual unit-ID into the memory. This feature allows to analyse the transmitted radar pulses in detail. Figure 2 shows pulses from the X-SAR recorded by a ground calibration receiver. The almost perfect rectangular-shaped pulses gave us a first indication of the good performance of the X-SAR transmit path including the antenna.

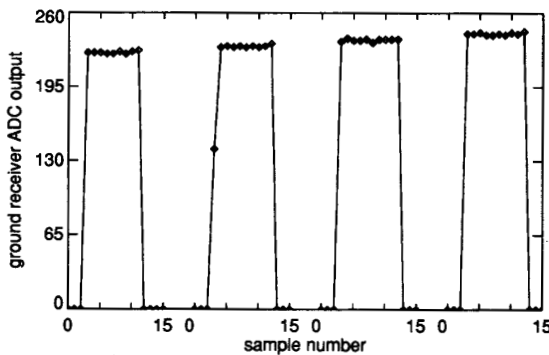


Figure 2: X-SAR pulses recorded by a ground calibration receiver

Special algorithms based on an integration of the measured pulses provide the received power versus time of receipt, i.e. due to the platform motion an azimuth cut through three-dimensional pattern. An example X-SAR azimuth pattern is presented in figure 3. It was recorded at the swath center and gives a maximum received power of -35.3 dBm, which corresponds to a ground flux density of -9.7 dBm/m², as expected. The azimuth pattern shows symmetric side lobes, a further indication that the antenna works well.

From all azimuth cuts we derived the maximum received power. We then used the slant range and off-nadir look angle of every receiver location, provided by JPL's orbit software package EGEN/DTOG, to apply the range correction and to end up with the elevation pattern shown in figure 4. The crosses mark the receiver measurements and the solid line is a polynomial fit of order four to these measurements. This results are in good agreement with the reconstructed (preflight measured) elevation pattern shown as a dashed line.

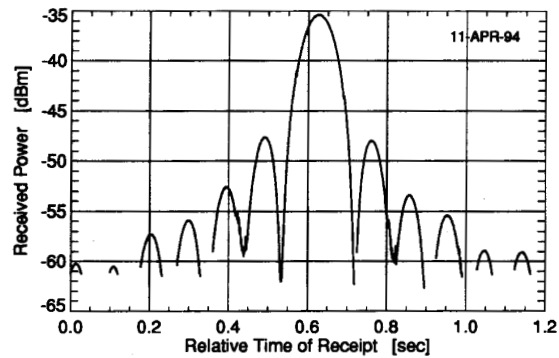


Figure 3: X-SAR azimuth antenna pattern recorded by a ground calibration receiver

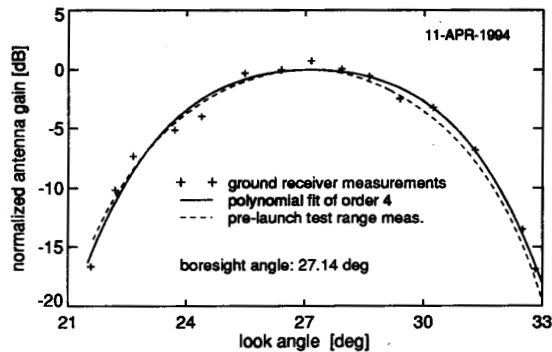


Figure 4: X-SAR elevation antenna pattern derived from ground calibration receiver measurements (data take 30.0)

The other information necessary for antenna pattern correction is the antenna boresight. Uncertainties in boresight angle determination are one of the major error sources in overall calibration. The maximum of our polynomial fit in figure 4 indicates a boresight angle of 27.14 deg.

Further results including L- and C-band antenna patterns and beam alignment measurements will be presented at the symposium.

ABSOLUTE RADIOMETRIC CALIBRATION

For the purpose of absolute radiometric calibration we deployed 15 trihedral corner reflectors of different size (six with 3 m, six with 1.5 m and 3 with 1 m leg length). The trihedrals have been reoriented to the shuttle path before each data take. Using our antenna elevation pattern from figure 4 and the corresponding boresight angle our colleagues from the German PAF (Processing and Archiving Facility) could process the first radiometrically corrected X-SAR image.

We analysed this image on a calibration work station using our analyses software package CALIX. 10 of our trihedrals were imaged on this data take. The calibration factors found from the



Figure 6: X-SAR image of the Oberpfaffenhofen test site, no radiometric corrections applied

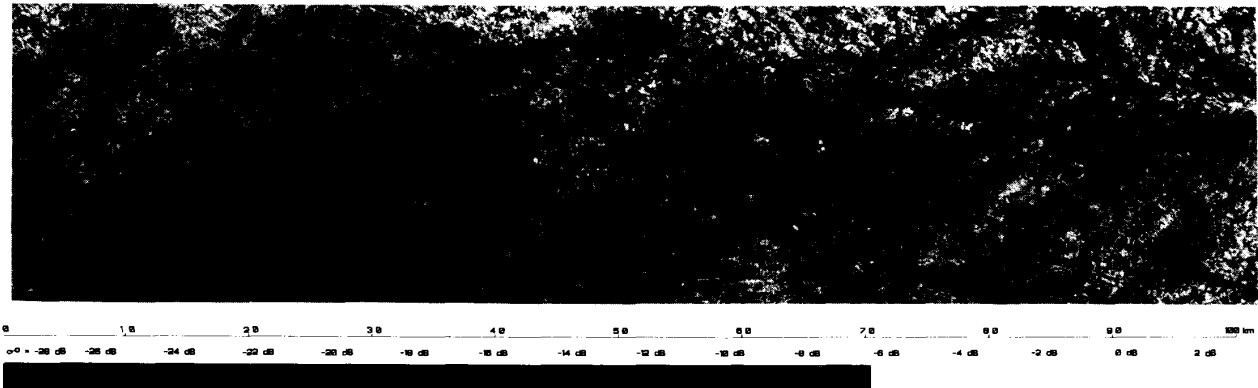


Figure 7: First calibrated X-SAR image (data take 30.0)

individual trihedrals are marked as asterisks in figure 5. The average calibration factor is 57.3 dB with a low standard deviation of 0.4 dB. Backscattering coefficients of the surrounding background clutter were lower than -10 dB. Figure 7 shows this first calibrated X-SAR image. The center of the image shows the area of DLR and the neighbouring airfield. Our corner reflectors can be recognized as white crosses between DLR and the lakes to the left. The gray tone scale at the bottom of the image shows the conversion from gray levels to backscattering coefficients. Figure 6 is the same image without corrections. The effect of the radiometric corrections is clearly visible, especially in near and far range.

ACKNOWLEDGMENT

I acknowledge the contribution and support of 30 colleagues (the X-SAR calibration team) to the Oberpfaffenhofen calibration campaign. The mission operations team in the POCC provided the necessary information on the system settings and the shuttle orbit. Special thanks goes to the D-PAF for their cooperation and the precision processing of calibration scenes.

REFERENCES

- Alenia Spazio, "PM-Antenna Electrical Test Report," *TR/X-SAR/2700/SS-04*, Rome, Italy, Feb. 1991.
- Bamler R. and M. Eineder, "X-SAR Precision Processor Calibration," *Technical Note, Version 2.0*, DLR, Oberpfaffenhofen, May 1993.

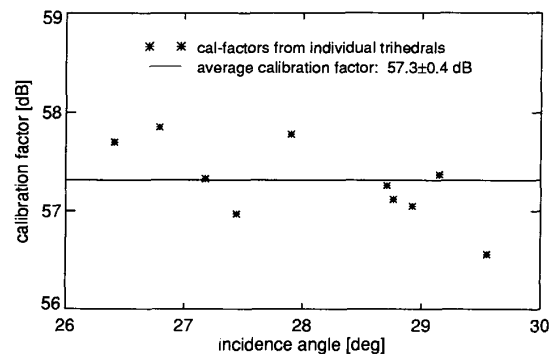


Figure 5: X-SAR absolute calibration factor derived from data of the first overflight (data take 30.0)

- Jordan, R.L., B.L. Huneycutt and M. Werner, "The SIR-C/X-SAR Synthetic Aperture Radar System," *IEEE Proc.*, Vol. 79, No. 6, June 1991, pp. 827-838.
- Seifert P., H. Lentz, M. Zink and F. Heel, "Ground-Based Measurements of Inflight Antenna Patterns for Imaging Radar Systems," *IEEE TGARS*, Vol. 30, No. 6, Nov. 1992, pp. 1131-1136.
- Zink M., "The X-SAR Calibration Plan: Part I and II," DLR, Technical Report, Oct. 1993.